29. Rowan-Robinson, M. *Mon. Not. R. astr. Soc.* (in the press).
30. Zeldovich, Ya. B. & Novikov, I. D. *Relativistic Astrophysics* Vol. 1 (University of Chicago Press, 1971).
31. Fricke, K. J. *Astrophys. J.* **183**, 941–958 (1973).
32. Negroponte, J., Rowan-Robinson, M. & Silk, J. *Astrophys. J.* **248**, 38–46 (1981).
33. French, H. B. *Bull. Lick Obs.* No. 863 (1979).
34. Lequeux, J., Peimbert, M., Rayo, J. F., Serrano, A. & Torres-Peimbert, S. *Astr. Astrophys.* **80**, 155–166 (1979).
35. Kunth, D. in *Cosmology and Particles* (eds Audouze, J. *et al.*) 241 (Frontiéres, Paris 1981).
36. Yang, J., Schramm, D. N., Steigman, G. & Rood, R. T. *Astrophys. J.* **227**, 697–704 (1979).
37. Wagoner, R. V. *Astrophys. J.* **179**, 343–360 (1973).
38. Olive, K. A., Schramm, D. N., Steigman, G., Turner, M. S. & Yang, J. *Astrophys. J.* **246**, 557–568 (1981).
39. Bondarenko, L. N., Kurguzov, V. V., Prokof'ev, Yu. A., Rogov, E. V. & Spivak, P. E. *JEPT Lett.* **28**, 303–306 (1978).
40. Wilkinson, D. H. in *Proc. of the Erice School on Nuclear Astrophys* (1980).
41. Cowsik, R. in *Cosmology and Particles* (ed. Adouze *et al.*) 157 (Frontiéres, Paris, 1981).
42. Carr, B. J. *Astr. Astrophys.* **60**, 13–26 (1977).
43. Epstein, R. I. *Astrophys. J.* **212**, 595–601 (1977).
44. Wright, E. L. *Astrophys. J.* **255**, 401–407 (1982).
45. Rana, N. C. *Mon. Not. R. astr. Soc.* **197**, 1125–1138 (1981).
46. Adouze, J. & Tinsley, B. M., *Ann. Rev. Astr. Astrophys.* **14**, 43–79 (1976).
47. Truran, J. W. & Cameron, A. G. W. *Astr. Space Sci.* **14**, 179–222 (1971).
48. Hartquist, T. W. & Cameron, A. G. W. *Astr. Space Sci.* **48**, 145–158 (1977).
49. Bond, H. E. *Astrophys. J.* **248**, 606–611 (1981).
50. Klapp, J. thesis, Univ. Oxford (1982).

Vitrification of pure liquid water by high pressure jet freezing

Erwin Mayer & Peter Brüggeller

Institut für Anorganische und Analytische Chemie, Universität Innsbruck, A 6020 Innsbruck, Austria

The vitrification of pure liquid water by projecting a thin jet of liquid water at high speed into a liquid cryomedium is reported. The influence of the experimental parameters on the cooling rate and the devitrification of the jet-frozen vitrified material have been investigated. A structural difference between vitrified liquid water and amorphous solid water prepared from the vapour phase is inferred from a comparison of the X-ray diffraction patterns.

FINDING a method for vitrifying pure liquid water is important for several reasons. The investigation of vitrified liquid water will help to elucidate the structure of liquid water because the effects of thermal and static disorder can be largely separated[1–4]. It might help in interpreting the anomalous properties of supercooled water[5–8]. Vitrification of biological systems without cryoprotectants is another application that could enable studies to be made of morphology without freezing artefacts and of the mechanism of freezing damage[9,10]. When applied to dilute aqueous solutions complete vitrification means the simultaneous matrix isolation of dissolved species. This extends the well known matrix isolation from the gas phase[11] to nonvolatile solutes such as ionic systems or biomolecules and allows, among others, spectroscopic investigations at low temperatures in the dissolved state. Attempts to form vitreous ice by rapid cooling of liquid water have invariably led to formation of ice I_h (ref. 12). (Pryde and Jones[13] did report a heat capacity change of rapidly cooled water at 126 K which they attributed to a glass transition, but could not reproduce this result in subsequent experiments.) We have recently described the complete vitrification of liquid water and dilute aqueous solutions by jet-freezing of aqueous droplets distributed in *n*-heptane as an emulsion, where the combination of emulsification and high cooling rate was essential for vitrification[14]. We have since increased the cooling rate by orders of magnitude and report here the vitrification of pure liquid water without emulsification by injecting a thin fluid jet of liquid water at high pressures *in vacuo* into a liquid cryomedium. This is an extension of the jet-freezing method developed by Bachmann and Schmitt for freeze etching[15]. Our technique differs from that of splat-cooling on a cold metal surface by using a liquid cryomedium, and gives for liquid water and dilute aqueous solutions much higher cooling rates[14]. [It has been reported that D. R. Uhlmann has vitrified liquid water by splat-quenching (ref. 16 in our ref. 6). However, to our knowledge no report has appeared since then.]

Conditions for vitrification

We have investigated the following parameters, considered to be important for a high cooling rate, with the ESR method described previously[14]: aperture diameter from 5 to 100 μm, working pressures between 10 and 400 atm, effect of the liquid cryomedium and of stirring. Small aperture diameter together with high working pressure were found to be most important for high cooling rates. With increasing working pressures the liquid jet is broken up by air resistance closer and closer to the exit hole of the aperture and dispersed into a fine mist. Therefore vacuum is essential for working at pressures above 100 atm. Liquid ethane, propane and butene-1 were investigated as cryomedia and gave for small apertures very similar cooling rates. Figure 1*a* shows the X-ray diffraction pattern of a jet-frozen sample of liquid water using the best conditions for vitrification emerging from hundreds of experiments: jetting through a 10-μm aperture with 400 atm working pressure (the

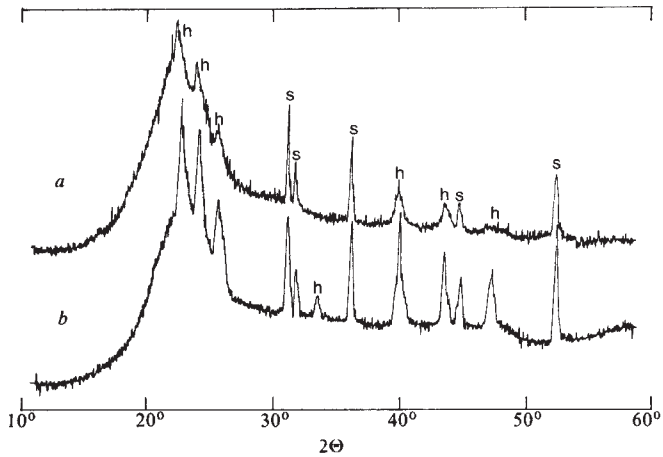

Fig. 1 X-ray diffraction patterns (CuKα, 90 K) of jet-frozen pure liquid water with: *a*, 400 atm; *b*, 100 atm working pressure (s, substrate reflexes; h, reflexes from crystalline ice). Samples were jet-frozen as follows: between 2 and 5 ml of pure liquid water were jetted through an aperture with a 10-μm opening (Balzers Union no. 16001), using working pressures of at most 400 atm, into 120 ml of vigorously stirred liquid propane cooled to 80 K. Liquid consumption at 100 atm: 0.4 ml min^{-1}, at 400 atm: 1.1 ml min^{-1}. The working pressures were generated with a hydraulic pump (type Maximator MSF 72), plugging of the 10-μm aperture was prevented by two filters (a Nupro 2-μm metal filter and a Millipore high pressure filter unit with a 0.2 μm filter). The experiment was started at normal pressure and vacuum applied as quickly as possible. Starting and stopping the jet already *in vacuo* gave identical X-ray diffraction patterns, but seemed to give apertures that clogged more easily. The suspension was filtered at liquid nitrogen temperature and the remaining mixture of frozen water and liquid cryomedium was transferred quickly with a liquid-nitrogen cooled spoon into the precooled apparatus. All operations at normal pressure were carried out under a cover of dry nitrogen gas. At liquid-nitrogen temperatures special care has to be taken to prevent accumulation of liquid oxygen in the cryomedium. The X-ray data were recorded on a Kristalloflex 4 (Siemens), using a vertical flat sample holder and samples between 0.5 and 1 mm thick.

0028–0836/82/330715—04$01.00

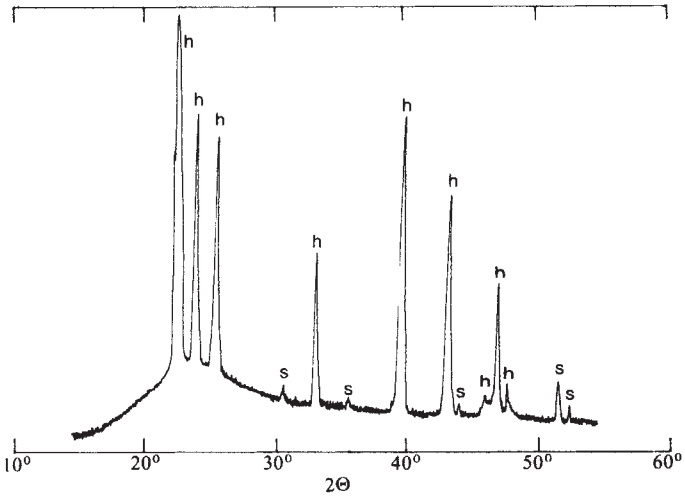

Fig. 2 X-ray diffraction pattern (CuKα, 90 K) of jet-frozen pure liquid water with 10 atm working pressure, showing the contribution of the liquid cryomedium at $2\theta = 23°$ (s, substrate reflexes; h, reflexes from ice I_h). The experimental conditions and the instrument gain were the same as conditions for Fig. 1 except for the working pressure and an aperture with a 20-μm opening. A 20-μm aperture was used because we could not start the jet through a 10-μm aperture with only 10 atm working pressure. However, from jet-freezing experiments with 50 atm we know that apertures with 10 and 20 μm openings give comparable cooling rates in this range of working pressures. With 10 atm working pressure the comparatively slow jet is not broken up by air over a long distance and thus the cooling rate is not increased by jetting *in vacuo*. The sharp reflexes are due to ice I_h, the intensity changes at small angles being caused by texture.

highest pressure used) into vigorously stirred propane at 80 K *in vacuo*. The X-ray diffraction pattern contains only a small amount of crystalline—mainly hexagonal—ice and is dominated by the broad feature characteristic of vitreous or microcrystalline substances. The effect of high working pressures is clearly seen by comparison with Fig. 1*b* where the pressure was reduced to 100 atm, using otherwise jet-freezing conditions identical with the experiment of Fig. 1*a*, and where the amount of hexagonal ice increases strongly. In several experiments we obtained nearly identical X-ray diffraction patterns with the same set of jet-freezing conditions which means that this method of vitrification is highly reproducible.

The vitrified liquid water inevitably contains some liquid cryomedium which cannot be removed without partial devitrification. The effect of the liquid cryomedium on the X-ray diffraction pattern of vitrified liquid water is demonstrated by Fig. 2, where the pattern of jet-frozen water using 10 atm working pressure only is shown with approximately the same intensity as in Fig. 1*a*, *b*: by differential thermal analysis (DTA) and by the ESR method reported previously[14] we confirmed that jet-freezing with 10 atm working pressure gives only crystalline ice. The X-ray diffraction pattern contains a broad peak centred at $2\theta = 23°$ in addition to the strong reflexes of ice I_h and is very similar to the pattern of a mixture of the liquid cryomedium with crystalline ice. The broad peak in Fig. 2 is therefore caused by the liquid cryomedium[16] and not by vitrified liquid water. The comparatively strong X-ray intensity of the liquid hydrocarbon might at first seem surprising. The small absorption coefficient for X rays of the solid water and the resulting transparency of the sample provide a simple explanation. In addition a matrix effect of the liquid cryomedium leading to strongly enhanced Compton scattering[17] and a particle size effect[18] might have a role. In any case the jet-freezing conditions for Fig. 2 are useful as a 'null-experiment', showing clearly in comparison with Fig. 1 the effect of high working pressures on the relative X-ray intensities of crystalline and amorphous material. We do not consider it useful to correct the X-ray diffraction pattern of vitrified liquid water for the effect of the cryomedium quantitatively because the amount of liquid and thus the size of the broad peak in Fig. 2 varied somewhat, and the possible additional effects considered above cannot be evaluated.

The vitrified material is definitely liquid water and not water vapour because: (1) the liquid enters the cryomedium as a continuous fluid jet of ~10 μm diameter. Typically between 2 and 5 ml of liquid water were jetted using a vacuum of 1 torr total pressure. The jetting time depends on the working pressure and the diameter of the aperture and was varied between 1 and 5 min. Therefore the amount of water vapour present during the experiment is negligible in comparison to the total amount of liquid water jetted. (2) We had tried to vitrify liquid water in the form of a very fine mist of small water droplets using working pressures of 1 to 2 atm only. The water droplets were generated by an ultrasonically vibrating 10-μm orifice similar to the aerosol generator of Berglund and Liu[19]. These experiments were carried out with a very small flow rate over considerable periods of time and therefore represent conditions where the amount of water entering the liquid cryomedium from the vapour phase becomes increasingly important. However, we have found no indication that material was vitrified using this arrangement. (3) The ESR spectra of jet-frozen 0.10 M aqueous $CuCl_2$ solutions depend strongly on the working pressures and were used as a good indicator for relative cooling rates[14]. We found that with a 200-atm working pressure the jet-frozen ESR spectrum is already nearly identical to the ESR spectrum of a perfectly vitrified 0.10 M $CuCl_2$ solution containing 50% glycerol for vitrification. While this does not prove that the jet-frozen solid has been vitrified completely, it still proves that the solute $CuCl_2$ has been matrix isolated and hence, that the liquid has experienced very high cooling rates.

Our jet-freezing conditions give a clear improvement, in terms of the amount of the vitrified material, over the previously reported vitrification of emulsified liquid water droplets[14] where we had obtained yields of ~13 and 16% for pure water and a 0.10 M $CuCl_2$ solution by DTA. These yields had been only barely noticeable in the X-ray diffraction pattern as a broadening underneath the sharp reflexes of the crystalline material between $2\theta = 20°$ and 28° (see Fig. 1*a* in ref. 14), whereas in Fig. 1*a* we have only a small amount of crystalline material on top of the broad feature. The determination of the relative amount of vitrified liquid water by DTA does not have any meaning for samples prepared as described in Fig. 1*a*, because the DTA method is not accurate enough, and the crystalline material comes mainly from condensation of water vapour during the preparation and transfer of the sample to the X-ray camera.

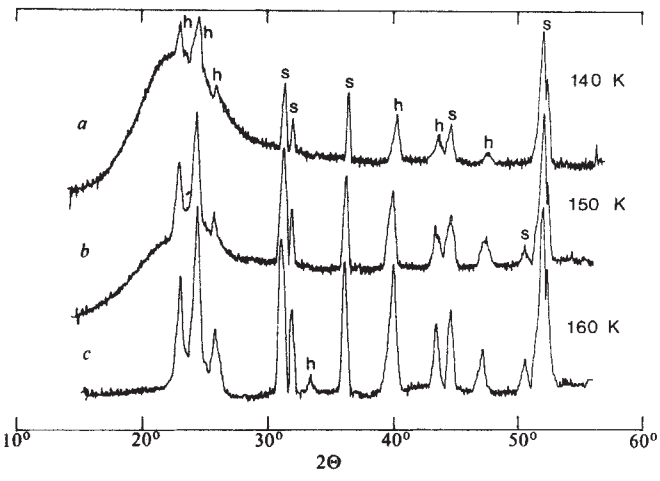

Fig. 3 X-ray diffraction patterns (CuKα) of jet-frozen pure liquid water warmed consecutively for 30 min to *a*, 140 K; *b*, 150 K; *c*, 160 K. The sampe was prepared as described in Fig. 1 with 400 atm working pressure except that liquid butene-1 was used as cryomedium at 100 K instead of propane. From 90 to 140 K the relative intensities of amorphous to crystalline reflexes were approximately constant, only the overall intensity decreased, probably due to movement of the viscous paste on the vertical sample holder with increasing temperature.

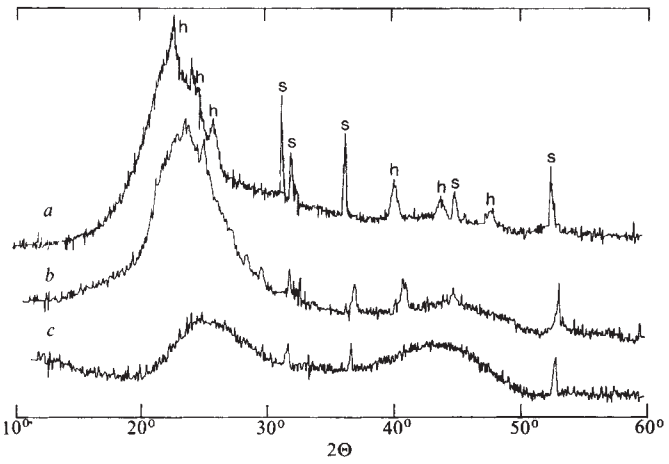

Fig. 4 X-ray diffraction patterns (CuKα, 90 K) of: *a*, jet-frozen pure liquid water prepared as described for Fig. 1*a* and thus containing some liquid propane; *b*, $(H_2O)_{as}$ mulled with liquid propane; *c*, $(H_2O)_{as}$ without propane. $(H_2O)_{as}$ was prepared as described in ref. 22 by vapour condensation at 77 K on a Cu-plate from a bath for the reservoir of water held at 210 K, using high vacuum conditions. For comparison with the pattern in Fig. 4*a* $(H_2O)_{as}$ was mixed thoroughly at 80 K with 20 ml of liquid propane, filtered and the remaining paste transferred to the precooled apparatus, using the same technique as for jet-frozen liquid water samples. As the pattern of $(H_2O)_{as}$ in Fig. 4*c* contains no reflexes of crystalline impurities, the amount of crystalline material in Fig. 4*b* represents the contamination of vitrified samples by crystalline ice due to condensation of water vapour during the experimental procedure.

We have investigated the devitrification and found that within the time scale of our X-ray measurements (30 min at every consecutive 10 K, starting at 90 K) the formation of ice I_c starts at 150 K (Fig. 3). This agrees very well with the devitrification of a vitrified 0.10 M $CuCl_2$ solution investigated previously within a similar time scale using ESR where a devitrification temperature of 153 K was deduced from signal broadening[14]. We found that the cryomedium used for vitrification affects the devitrification temperature. The sample giving the X-ray diffraction patterns in Fig. 3 had been prepared by jetting liquid water into butene-1 and therefore contained some butene-1. Vitrified liquid water containing some propane had started to devitrify already at 130 K. We think that this difference comes from the higher vapour pressure of liquid propane (1 torr at 144 K) and that devitrification is possibly induced by evaporating propane. At low temperatures the X-ray diffraction patterns of vitrified samples prepared with butene-1 or propane as cryomedia, using otherwise identical jet-freezing conditions, are very similar. The X-ray diffraction patterns of jet-frozen samples stored at 77 K for 3 months did not show any change.

Comparison with $(H_2O)_{as}$

In Fig. 4 the X-ray diffraction pattern of vitrified liquid water containing some liquid propane (Fig. 4*a*) is compared with the pattern of amorphous solid water prepared by condensation from the vapour phase (called $(H_2O)_{as}$ in accordance with Rice[1], Fig. 4*b*, *c*). Figure 4*c* shows the published X-ray diffraction pattern of $(H_2O)_{as}$ (refs 3, 20). Figure 4*b* the pattern of $(H_2O)_{as}$ mulled with liquid propane. A comparison has meaning only between the patterns of samples treated both with liquid cryomedium and has to be made between the patterns shown in Fig. 4*a*, *b*. A difference might possibly be found at high angles where the broad feature in the pattern of $(H_2O)_{as}$ centred around $2\theta = 44°$ appears to be less intense or absent in the pattern of vitrified liquid water. For further comparison we have tried to remove the cryomedium by washing the sample with liquid methane. However, this procedure leads to partial devitrification of the sample. In Fig. 5 the X-ray diffraction pattern of vitrified liquid water washed with liquid methane (Fig. 5*b*) is compared with the pattern of $(H_2O)_{as}$ treated identically (Fig. 5*a*), showing again for vitrified liquid water no clear amorphous peak at $2\theta = 44°$ underneath the sharp reflexes of crystalline ice in contrast to the pattern of $(H_2O)_{as}$. The X-ray diffraction pattern of the devitrified sample in Fig. 5*c* can be used as background of Fig. 5*b*. However, only a presentation of the X-ray data in the form of the structurally sensitive part of the scattered X-ray intensity will make a clear differentiation possible, and we cannot do this because we have not been able to compensate for the effect of the liquid cryomedium.

Discussion

The influence of high working pressures on the amount of vitrified material and thus on the cooling rate is certainly connected with the speed of the liquid jet. For 10, 100 and 400 atm working pressures approximate jet speeds of 20, 100 and 250 m s^{-1} can be calculated from the diameter of the 10-μm aperture and consumption of liquid. The effect of jet speed can be easily demonstrated by jetting at room temperature into paraffin oil with a viscosity similar to liquid propane at 80 K. With 10 atm working pressure the liquid jet hardly penetrates the surface, whereas with 100 atm working pressure penetration goes up to 20–30 mm. Therefore the liquid jet passes within a given time with increasing jet speed a larger volume of cryomedium, causing more efficient heat transfer from water to the cryomedium and giving higher cooling rates. In addition, vigorous stirring of the cryomedium enforces a circular movement onto the liquid jet, probably breaking up the jet into small droplets.

It is impossible to measure the cooling rates obtainable with high pressure jet-freezing. Fletcher[12] estimated the cooling rate necessary for vitrifying a micrometre-sized droplet of water to be $>10^{10}$ K s^{-1} from the theory of the homogeneous nucleation of freezing, whereas Uhlmann[21] calculated a cooling rate of $>10^7$ K s^{-1}. We do not know how the liquid jet breaks up in the cryomedium at high pressures, but we consider it likely that the jet breaks up into droplets of approximately the size of the jet diameter. Therefore a minimum cooling rate of 10^{10} K s^{-1} is obtained from Fletcher's value and of 10^7 K s^{-1} from Uhlmann's. As the minimum cooling rate depends strongly on droplet diameter and was calculated for 1-μm droplets[12,21] much higher cooling rates would result for larger droplet diameters. For a 10-μm droplet minimum cooling rates of 10^{13} and 10^{10} K s^{-1} follow from Fletcher's and Uhlmann's calculations. An idea about the distribution of cooling rates can be obtained from an inspection of the frozen products. We had

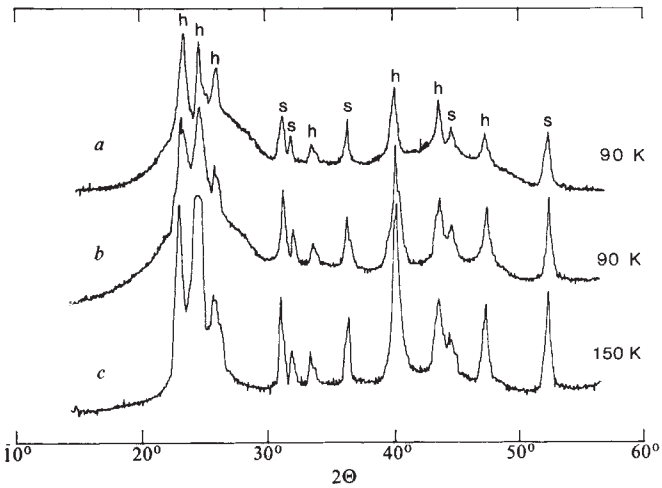

Fig. 5 X-ray diffraction patterns (CuKα) of: *a*, $(H_2O)_{as}$ from Fig. 4*b* washed with liquid methane; *b*, jet-frozen liquid water from Fig. 4*a* washed with liquid methane; *c*, the sample in *b* devitrified by warming up to 150 K. To remove liquid propane or butene-1 the samples were washed with liquid methane, filtered at ~90 K as described in Fig. 1 for propane, and the remaining methane pumped off at 77 K from the sample. This procedure leads inevitably to strong contamination and/or partial devitrification of the samples as shown by a comparison of Fig. 5*a* with Fig. 4*b* and *c*. The reflex at $2\theta = 24.3°$ in Fig. 5*c* was truncated.

expected that with increasing working pressure, increasing amounts of ice I_c and then of vitrified liquid water would be formed. This was frequently observed for the preparation of $(H_2O)_{as}$ from the vapour phase[20,22]. However, Fig. 1*b* shows that the crystalline fraction consists mainly of ice I_h in addition to the vitrified material. Thus the liquid jet apparently experiences either low cooling rates, giving ice I_h, or very high cooling rates leading to vitrified water. We believe that this is due to the vortex of the vigorously stirred cryomedium.

The thermodynamic conditions necessary for vitrifying liquid water have been discussed recently by Angell and Tucker[8]. The argument is based on the incompatibility of an extrapolated value of the glass transition temperature of vitrified liquid water with Kauzmann's entropy paradox[23] which states that a liquid can be supercooled only by a limited number of degrees before it loses all its excess entropy over the crystal, that is before its total entropy becomes equal to that of the crystal. This presents a problem, especially for liquid water, because in supercooled water a drastic increase of C_p occurs with decreasing temperature[5] among other anomalies. To resolve the entropy paradox Angell and co-workers postulated the existence of a λ-type heat capacity anomaly at 228 K associated either with some liquid state mechanical instability or with the cooperative formation of a long-range hydrogen-bonded network with decreasing temperature[6–8]. Angell and Tucker speculate that liquid water departs during cooling (assuming a rate of 10^8 K s^{-1}) from the metastable heat capacity already below the maximum observed value (which has been recorded at 235 K (refs 6, 24)) due to the 'freezing out' of the 'anomalous fluctuations' (see Fig. 5 in ref. 8). From the C_p versus temperature curve we wonder whether liquid water does not diverge at much higher temperatures—thereby avoiding the anomalous C_p increase altogether—and lose its internal equilibrium than that suggested by Angell and Tucker, considering the extreme cooling rates discussed above. In analogy to SiO_2 the vitrified solid is supposed to have different densities depending on the temperature at which internal equilibrium was established before quenching[25,26]. However, a determination of the density of vitrified liquid water is not possible at present due to the presence of the liquid cryomedium.

The similarity of structure between vitrified liquid water and $(H_2O)_{as}$ has been disputed recently. Rice[1,3,27] and Angell[8] believe that there is a continuity of state between liquid water and $(H_2O)_{as}$, that $(H_2O)_{as}$ is essentially liquid water, especially because the observed glass transition temperature of $(H_2O)_{as}$ is identical with the extrapolated value for vitrified liquid water. This hypothesis is the basis of the random network model of water recently proposed by Rice *et al.*[4,28]. In contrast Johari[29] argues on thermodynamic grounds mentioned above that a discontinuity of states exists, and that therefore "the structure of $(H_2O)_{as}$ is different from the one towards which supercooled water would tend". We have tried without success to observe a glass transition temperature in our vitrified water samples. A structural difference between vitrified liquid water and $(H_2O)_{as}$ could possibly emerge from a comparison of the X-ray diffraction patterns (see Figs 4 and 5). We do not know yet if the absence of the broad peak at $2\theta = 44°$ in vitrified liquid water is real or is only an artefact caused by the presence of the liquid cryomedium. According to Narten and Levy[30] a change of the double maximum in the structure functions of liquid water around 2.5 $Å^{-1}$ into a single peak corresponds to a disappearance of the maxima and minima between 3.5 and 8 Å in the correlation functions.

We thank Professor E. Schnell for help with the X-ray work.

Received 10 December 1981; accepted 10 May 1982.

1. Olander, D. S. & Rice, S. A. *Proc. natn. Acad. Sci. U.S.A.* **69**, 98–100 (1972).
2. Rice, S. A. & Sceats, M. G. *J. phys. Chem.* **85**, 1108–1119 (1981).
3. Narten, A. H., Venkatesh, C. G. & Rice, S. A. *J. chem. Phys.* **64**, 1106–1121 (1976).
4. Rice, S. A. *Topics curr. Chem.* **60**, 109–200 (1975).
5. Angell, C. A. in *Treatise on Water* Vol. 7 (ed. Franks F.) (in the press).
6. Angell, C. A., Shuppert, J. & Tucker, J. C. *J. phys. Chem.* **77**, 3092–3099 (1973).
7. Speedy, R. J. & Angell, C. A. *J. chem. Phys.* **65**, 851–858 (1976).
8. Angell, C. A. & Tucker, J. C. *J. phys. Chem.* **84**, 268–272 (1980).
9. Mazur, P. *Science* **168**, 939–949 (1970).
10. Wolstenholme, G. E. W. & O'Connor, M. *The Frozen Cell* (Churchill, London, 1970).
11. Becker, E. D. & Pimentel, G. C. *J. chem. Phys.* **25**, 224–228 (1956).
12. Fletcher, N. H. *Rep. Prog. Phys.* **34**, 913–994 (1971).
13. Pryde, J. A. & Jones, G. O. *Nature* **170**, 685–688 (1952).
14. Brüggeller, P. & Mayer, E. *Nature* **288**, 569–571 (1980).
15. Bachmann, L. & Schmitt, W. W. *Proc. natn. Acad. Sci. U.S.A.* **68**, 2149–2152 (1971); in *Freeze Etching* (eds Benedetti, E. L. & Favard, P.) 73–79 (Soc. Frac. Microsc. Electron, Paris 1973).
16. Stewart, G. W. & Mannheimer, M. *Z. anorg. allg. Chem.* **171**, 61–72 (1928).
17. Sahores, J. J. *Adv. X-ray Analysis* **16**, 186–197 (1973).
18. Berry, P. F., Furuta, T. & Rhodes, J. R. *Adv. X-ray Analysis* **12**, 612–632 (1969).
19. Berglund, R. N. & Lui, B. Y. H. *Envir. Sci. Technol.* **7**, 147–153 (1973).
20. Dowell, L. G. & Rinfret, A. P. *Nature* **188**, 1144–1148 (1960).
21. Uhlmann, D. R. *J. Non-Cryst. Solids* **7**, 337–348 (1972).
22. Hobbs, P. *Ice Physics* (Clarendon, Oxford, 1974).
23. Kauzmann, W. *Chem. Rev.* **43**, 219–256 (1948).
24. Rasmussen, D. H., MacKenzie, A. P., Tucker, J. C. & Angell, C. A. *Science* **181**, 342–344 (1973).
25. Kanno, H. & Angell, C. A. *J. chem. Phys.* **73**, 1940–1947 (1980).
26. Bruckner, R. *J. Non-Cryst. Solids* **5**, 281 (1971).
27. Rice, S. A., Bergren, M. S. & Swingle, L. *Chem. Phys. Lett.* **59**, 14–16 (1978).
28. Rice, S. A. & Sceats, M. G. *J. phys. Chem.* **85**, 1108–1119 (1981).
29. Johari, G. P. *Phil. Mag.* **35**, 1077–1090 (1977).
30. Narten, A. H. & Levy H. A. *J. chem. Phys.* **55**, 2263–2269 (1971).

The molecular basis of DNA–protein recognition inferred from the structure of cro repressor

D. H. Ohlendorf*, W. F. Anderson†, R. G. Fisher*, Y. Takeda‡ & B. W. Matthews*

*Institute of Molecular Biology and Department of Physics, University of Oregon, Eugene, Oregon 97403, USA
†MRC Group on Protein Structure and Function, Department of Biochemistry, University of Alberta, Edmonton, Alberta, Canada T6G 2H7
‡Chemistry Department, University of Maryland, Baltimore County, Catonsville, Maryland 21228, USA

Recognition by cro repressor protein of its specific DNA binding sites appears to occur via multidentate hydrogen bonds between amino acid side chains of the protein and base-pair atoms in the major groove of right-handed B-form DNA. Most of the sequence-specific interactions between cro and DNA, as well as a number of sequence-independent ones, are mediated by a two-α-helical unit which appears to be common to many proteins that regulate gene expression.

THE structures of three proteins that specifically bind to DNA have recently been determined, namely, the cro repressor protein (hereafter called 'cro') from bacteriophage λ[1], the catabolite gene activator protein (CAP) from *Escherichia coli*[2] and the amino-terminal fragment of the *c*I repressor protein (cI) from bacteriophage λ[3]. It has been proposed that these proteins bind to DNA with protruding α-helices penetrating[1,2] or partly penetrating[3] the major grooves of the DNA (in the case of CAP, the DNA has been postulated to be left-handed[2]).

In this article we propose a detailed model for the complex between cro and DNA. The model is consistent with the relative binding affinities of cro for the six operator sites within bacteriophage λ at which it binds specifically, and can also be used to rationalize known changes in binding affinity caused by mutations within these sites.

Cro is one of a number of proteins that participate in the

0028–0836/82/330718—06$01.00